XLIII CILAMCE
21–25, November, 2022
FOZ DO IGUAÇU – PR – BRAZIL

Numerical analysis of floating structures using a fluid-structure interaction model for free surface flows and anchored bodies

Mateus Guimarães Tonin[1], Gabriela Penna Bianchin[1], Alexandre Luis Braun[1]

[1]*Programa de Pós-Graduação em Engenharia Civil, Universidade Federal do Rio Grande do Sul*
Av. Osvaldo Aranha 99, 90035-190, Porto Alegre - RS, Brazil
mateus.tonin@ufrgs.br, gabriela_bianchin@hotmail.com, alexandre.braun@ufrgs.br

Abstract. The present work is dedicated to the numerical simulation of Fluid-Structure Interaction (FSI) problems involving floating bodies subjected to the action of free-surface flows, where the structure may or may not be anchored through mooring cables. The numerical model proposed here may be utilized in several practical applications, such as: ships hydro-aerodynamics, stability of oil extraction platforms, efficiency of wave energy converters, stability of floating bridges, floating houses and buildings. In the present model, the fluid equations are discretized using the Characteristic-Based Split (CBS) method in the context of the Finite Element Method (FEM). For the treatment of multiphase free-surface flows, the Level Set Method is used, where the fluid is considered as a biphasic medium. The structure is kinematically described using a rigid body approach and the mooring cable is modeled using an elastic material with geometric nonlinearity and the Nodal Position Finite Element Method (NPFEM). The system of equations of motion is discretized in time using the implicit Newmark and α-Generalized methods. Problems involving floating bodies with and without anchoring are simulated to demonstrate the applicability and accuracy of the proposed numerical model.

Keywords: Floating Structures; Fluid-Structure Interaction; Free-Surface Flows; Cable Dynamics.

1 Introduction

With the advances observed in the last decades in the technology of materials and construction methods, the so-called floating bodies have been increasingly used in different areas of Engineering. From vessels for the transport of cargo and passengers, through oil extraction platforms, to buildings, bridges and ports. For an adequate evaluation of the behavior of these structures, experimental and field studies are usually necessary, which unfortunately have high costs. An economical alternative would be the use of numerical simulation through a model that takes into account the interactions existing between the floating body and the fluid flows that surround it, including the action of wind, waves and water currents, in addition to the anchoring and foundation structures and their interaction with the water and marine soil, where the anchoring system is fixed.

This work aims at the development of numerical FSI tools for the analysis of bodies subject to the action of free surface flows. The main objective is to obtain a coupling model for future studies on the behavior of floating bodies subjected to simultaneous actions of wind and interaction of the body with the water, which may or may not be anchored through mooring cables.

The flow equations are discretized using the CBS method considering a semi-implicit scheme. For the turbulence treatment, it's employed the Large Eddy Simulation (LES) methodology, using the classical and dynamic Smagorinsky models for scales below mesh resolution. For the spatial discretization of the domain, the FEM is employed using linear tetrahedral elements. For the treatment of problems involving free surface flows, the Level Set method is implemented, considering the flow as a two-phase fluid medium (air and water). For the analysis of flows in the presence of moving bodies, an Arbitrary Lagrangian-Eulerian (ALE) formulation is used to describe the motion of fluid particles, with a mesh movement scheme proposed and implemented previously by Teixeira [1]. The solid body is treated in this work using a rigid body approach, considering 6 degrees of freedom. The temporal discretization is performed using the implicit Newmark and α-Generalized methods. For

the analysis of FSI problems, the explicit partitioned model is used. The numerical simulation of anchor cables is performed here using the NPFEM, working with positions as variables, rather than displacements. A special coupling scheme between cable rigid body is utilized in this work, which is based on the work by Sun et al. [2].

2 Formulation

2.1 Flow analysis and free surface modeling

In the present model, the flow is considered incompressible, consisting of a Newtonian fluid under isothermal condition and without mass or energy transport. Therefore, the Navier-Stokes equations and the mass balance form the system of flow equations. The Navier-Stokes equations are expressed using orthogonal Cartesian coordinates and arbitrary Lagrangian-Eulerian (ALE) kinematic description, i.e.:

$$\frac{\partial v_i}{\partial t} + \left(v_j - w_j\right)\frac{\partial v_i}{\partial x_j} = g_i - \frac{1}{\rho_f}\frac{\partial p}{\partial x_i} + \nu\frac{\partial^2 v_i}{\partial x_j^2} \qquad (i,j,k = 1,2,3), \tag{1}$$

where ρ_f is the specific mass of the fluid, v_i are the components of the flow velocity vector **v**, w_j are the components of the mesh velocity vector **w**, t denotes time, x_i are the components of the position vector **x** along the coordinate axes x_i, g_i are the components of the acceleration vector of gravity **g**, p is the thermodynamic pressure, δ_{ij} are the Kronecker delta components and ν is the kinematic viscosity coefficient.

The mass conservation equation can be expressed, considering an incompressible fluid, by the equation below:

$$\frac{\partial v_i}{\partial x_i} = 0 \qquad (i = 1,2,3). \tag{2}$$

For the free-surface flows, the Level Set method was adopted, where a signed distance function represented by the scalar ϕ is used, in such a way that the separation interface between fluids is located at positions where $\phi = 0$. In this way, one of the fluids assumes values $\phi < 0$ and the second takes on values $\phi > 0$. As an illustration, Fig. 1 shows an example involving rising bubbles in a fluid. The total area Ω is filled by a liquid region (where $\phi > 0$ was defined) and several gaseous regions ($\phi < 0$), with the interface ($\phi = 0$) represented by the lines Γ_F (Sussman et al. [3]). The equation describing the evolution of ϕ over time is given by (Sussman et al. [3]):

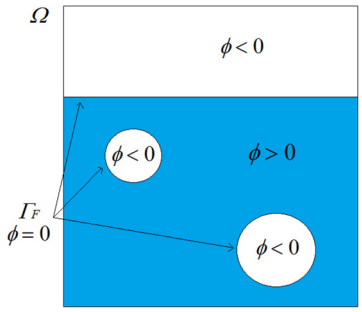

Figure 1. Level Set function to identify rising gas bubbles in a fluid

$$\frac{\partial \phi}{\partial t} + v_j\frac{\partial \phi}{\partial x_j} = 0 \qquad \left(j = 1,2,3\right). \tag{3}$$

The fluid physical properties are then defined as functions of ϕ, as shown in Eq. (4), while ρ_1 and ρ_2 are the fluid densities corresponding to fluids 1 and 2, respectively, and $H(\phi)$ is a "smoothed" Heaviside function, ε is the half-thickness of the transition zone, normally defined as $\varepsilon = \alpha_{LS}.\Delta x$, where Δx is the characteristic dimension of an element in the interface region and α_{LS} is a model parameter with values varying between 1 and 2.

$$\rho(\phi) = \rho_1 + (\rho_2 - \rho_1) H(\phi), \text{ being } H(\phi) = \begin{cases} 0 & \text{for } \phi < -\varepsilon \\ \frac{1}{2}\left[1 + \frac{\phi}{\varepsilon} + \frac{1}{\pi} sen\left(\frac{\pi\phi}{\varepsilon}\right)\right] & \text{for } |\phi| \le \varepsilon \\ 1 & \text{for } \phi > \varepsilon \end{cases}. \quad (4)$$

The numerical solution of Eq. 4 does not guarantee that ϕ will remain as a distance function (i.e. $|\nabla\phi| = 1$), thus a reinitialization procedure is necessary to ensure this condition (see Sussman et al. [4]). The flow problem is resolved here numerically using a semi-implicit CBS scheme in the context of the FEM, where linear tetrahedral elements are adopted for spatial discretization.

2.2 Cable analysis: NP-FEM formulation

Initially, consider the two-node straight cable element in a three-dimensional space, shown in Fig. 2. The element geometry is described by its nodal coordinates (X_i, Y_i, Z_i) (i=1, 2) in a global coordinate system $OXYZ$ and (x_i, y_i, z_i) (i=1, 2) in local coordinates x, y and z, where the x-axis is defined along the cable, y- and z-axes are perpendicular to the x-axis, respectively (Sun et al. [2]).

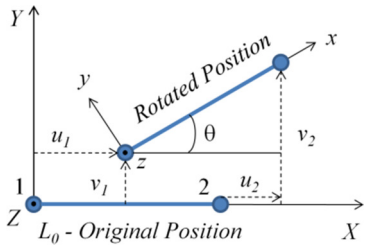

Figure 2. Straight cable element with two knots under rigid body motion

The position, velocity and acceleration of an arbitrary point along the cable element can be expressed in terms of element shape functions and the corresponding nodal values, in the form:

$$\mathbf{R} = \mathbf{N}\mathbf{X}_e, \quad \mathbf{v} = \dot{\mathbf{R}} = \mathbf{N}\dot{\mathbf{X}}_e, \quad \mathbf{a} = \ddot{\mathbf{R}} = \mathbf{N}\ddot{\mathbf{X}}_e, \; \mathbf{N} = \begin{bmatrix} 1-\zeta & 0 & 0 & \zeta & 0 & 0 \\ 0 & 1-\zeta & 0 & 0 & \zeta & 0 \\ 0 & 0 & 1-\zeta & 0 & 0 & \zeta \end{bmatrix}, \quad (5)$$

$$\zeta = \sqrt{(X - X_1)^2 + (Y - Y_1)^2 + (Z - Z_1)^2} \Big/ \sqrt{(X_2 - X_1)^2 + (Y_2 - Y_1)^2 + (Z_2 - Z_1)^2}, \quad (6)$$

where $\mathbf{R} = \{X, Y, Z\}^T$, $\mathbf{v} = \{v_x, v_y, v_z\}^T$ and $\mathbf{a} = \{a_x, a_y, a_z\}^T$ are the position, velocity and acceleration vectors of an arbitrary point in the global coordinate system, respectively, $\mathbf{X}_e = \{X_1, Y_1, Z_1, X_2, Y_2, Z_2\}^T$ is the global nodal coordinates at the current time, $\mathbf{N}$ is the element shape function matrix and dots denote time derivatives, respectively (Sun et al. [2]). In a total lagrangian description, deformation of the cable element is defined by $u = x - x_0$, being x_0 and x the coordinates of an arbitrary point along the element before and after deformation, respectively. The Green-Lagrange strain component ε_x at element level is defined as follows, where L and L_0 are the length of the deformed and undeformed element (Zhu [5]).

$$\varepsilon_x = \frac{L}{L_0} - 1 = \frac{X_2 - X_1}{L_0}\cos\theta_x + \frac{Y_2 - Y_1}{L_0}\cos\theta_y + \frac{Z_2 - Z_1}{L_0}\cos\theta_z - 1 = \mathbf{B}\mathbf{X}_e - 1. \quad (7)$$

2.3 Fluid-Structure Interaction

The floating body is modeled as a rigid body with six degrees of freedom, defined by the position of its center of gravity (CG), described by (X_b, Y_b, Z_b) in the global coordinate system, and also by its orientation, using Euler angles (θ_x – roll, θ_y – pitch, θ_z – yaw) in a body-fixed local coordinate system (x, y, z) with the origin

at the body CG, as shown in Fig. 3. The transformation order from the global to the local coordinate systems is defined as yaw, pitch and roll (Sun et al. [2]). A massless rigid cable element is used to link the moored body CG to the end of the cable, as shown in the figure.

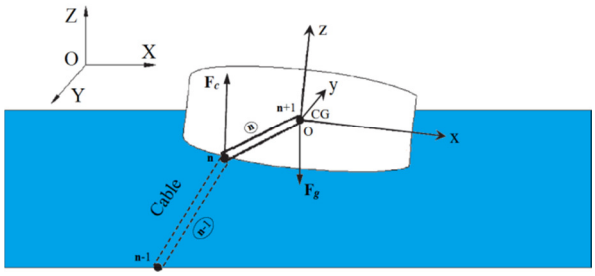

Figure 3. Schematic view of loads and coordinate systems of the moored body

The coupling of the fluid-cable-structure system can be performed by the following equation, at global level:

$$\begin{bmatrix} \mathbf{M}_c & \mathbf{0} & \mathbf{0} \\ \mathbf{0} & \mathbf{M}_b + \bar{\mathbf{M}}_S^{TT} & \bar{\mathbf{M}}_S^{TR} \\ \mathbf{0} & \bar{\mathbf{M}}_S^{RT} & \mathbf{A}^T\tilde{\mathbf{I}}\mathbf{A} + \bar{\mathbf{M}}_S^{RR} \end{bmatrix} \begin{Bmatrix} \ddot{\mathbf{X}}_C \\ \ddot{\mathbf{X}}_b \\ \ddot{\boldsymbol{\theta}} \end{Bmatrix} + \begin{bmatrix} \beta\mathbf{M}_c + \gamma\mathbf{K}_c & \mathbf{0} & \mathbf{0} \\ \mathbf{0} & \beta\mathbf{M}_b + \bar{\mathbf{C}}_S^{TT} & \bar{\mathbf{C}}_S^{TR} \\ \mathbf{0} & \bar{\mathbf{C}}_S^{RT} & \beta\mathbf{A}^T\tilde{\mathbf{I}}\mathbf{A} + \bar{\mathbf{C}}_S^{RR} \end{bmatrix} \begin{Bmatrix} \dot{\mathbf{X}}_C \\ \dot{\mathbf{X}}_b \\ \dot{\boldsymbol{\theta}} \end{Bmatrix} + \begin{bmatrix} \mathbf{K}_c + \mathbf{K}_{r1} & \mathbf{K}_{cr} & \mathbf{0} \\ \mathbf{K}_{cr}^T & \mathbf{K}_{r2} + \mathbf{K}_S^{TT} & \mathbf{K}_S^{TR} \\ \mathbf{0} & \mathbf{K}_S^{RT} & \mathbf{K}_S^{RR} \end{bmatrix} \begin{Bmatrix} \mathbf{X}_C \\ \mathbf{X}_b \\ \boldsymbol{\theta} \end{Bmatrix} = \begin{Bmatrix} \mathbf{F}_c \\ \bar{\mathbf{Q}}_S^b \\ \bar{\mathbf{Q}}_S^\theta \end{Bmatrix}, \tag{8}$$

where β and γ are Rayleigh damping parameters, $\mathbf{X}_C$ is a $3n$-dimension vector containing all the nodal coordinates of cable, n is total number of cable nodes, $\mathbf{X}_b$ and $\boldsymbol{\theta}$ are 3-dimension vectors containing the floating body CG position and rotation angles, respectively. $\mathbf{F}_c$ is the total external load vector acting on the cable. $\mathbf{K}_S$, $\bar{\mathbf{M}}_S$ and $\bar{\mathbf{C}}_S$ are the equivalent stiffness, mass and damping matrices (already with fluid contributions) related to the the floating body and $\bar{\mathbf{Q}}_S$ is the equivalent load vector, containing forces and moments generated by the fluid in addition to other forces and moments caused by the interaction between floating body and cable. $\mathbf{M}_c$ is the assembled global mass matrix of cable and $\mathbf{M}_b$ the mass matrix of the floating body. Similarly, $\mathbf{K}_c$, is the assembled global stiffness matrix of cable. The stiffness sub-matrices associated with the rigid cable element, $\mathbf{K}_{r1}$, $\mathbf{K}_{r2}$ and $\mathbf{K}_{cr}$, and the inertia tensor $\tilde{\mathbf{I}}$ are constructed as (Sun et al. [2]) follows, being (I_{xx}, I_{yy}, I_{zz}, I_{xy}, I_{yz}, I_{zx}) the components of the inertia tensor, evaluated at its CG at local coordinates. Finally, for the fluid-structure interaction, a conventional partitioned coupling scheme is used.

$$\mathbf{K}_{6\times6}^{rigid} = \mathbf{Q}^T\mathbf{K}_0\mathbf{Q} = \begin{bmatrix} \mathbf{K}_{r1(3\times3)} & \mathbf{K}_{r0(3\times3)} \\ \mathbf{K}_{r0(3\times3)}^T & \mathbf{K}_{r2(3\times3)} \end{bmatrix}_{6\times6}, \quad \mathbf{K}_{rr} = \begin{bmatrix} \mathbf{0}_{\mathbf{3(n-1)\times3(n-1)}} & \mathbf{0}_{\mathbf{3(n-1)\times3}} \\ \mathbf{0}_{\mathbf{(3\times3)(n-1)}} & \mathbf{K}_{r1(3\times3)} \end{bmatrix}_{3n\times3n},$$
$$\mathbf{K}_{cr} = \begin{bmatrix} \mathbf{0}_{\mathbf{3(n-1)\times3}} \\ \mathbf{K}_{r0(3\times3)} \end{bmatrix}_{3n\times3}, \quad \tilde{\mathbf{I}} = \begin{bmatrix} I_{xx} & -I_{xy} & -I_{xz} \\ -I_{xy} & I_{yy} & -I_{yz} \\ -I_{xz} & -I_{yz} & I_{zz} \end{bmatrix}. \tag{9}$$

3 Applications

3.1 Wave Packet Interacting with a Floating Body

Proposed by Hadžić et al. [6], the present problem studies the interaction of a floating body subject to a wave packet. Experimental results, conducted at the Technical University of Berlin, were obtained for a rectangular prism, 10 cm long, 5 cm high and 29 cm thick, with a density relative to water of 0.68 (Bouscasse et

al. [7]). Figure 4 presents a general scheme for the problem.

From Fig. 4, the flap-type wave-maker can be seen on the left edge. There is a distance of 2.11 m between the wavemaker and the floating body. The body has a mass of 0.986 kg and a moment of inertia of 1.4×10^{-3} kg.m². Given the large thickness of the body, the problem can be treated using a two-dimensional approach, using then three degrees of freedom. Also, Fig. 4 shows the time history of the flap wavemaker angle used to generate the wave packet. Its numerical representation in this work is given using velocity boundary conditions.

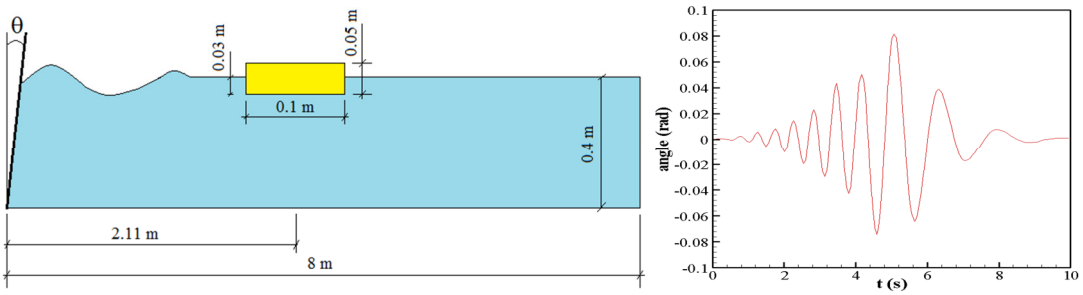

Figure 4. Wave packet interacting with floating body, general scheme (left) and time history of the wavemaker flap angle (right)

For the numerical simulation, a mesh of 528,039 tetrahedral elements and 176,634 nodes distributed in a non-linear manner was used. The smallest element dimension found is 1.82×10^{-3} m, located close to the fluid-structure interface. The boundary conditions used are free-slip walls on the right and bottom edges. The top edge has only zero pressure and the left edge has the velocities components *X* and *Y* prescribed in order to generate the wave packet for heights up to 0.6 m. From the height of 0.6 m, velocities components *X* and *Y* are imposed null.

Figure 5 presents the results obtained for heave (translation in *Y*) and roll (rotation in *Z*) of the floating body over time. Note that the results are similar to the experimental and numerical references, despite the numerical dissipation effect inherent to the Level Set method. For heave, it is noted that even at advanced time instants, such as t = 7.3 s, the response of the present work was very similar (relative error of 0.2%) to the experimental results of Hadžić et al. [6]; at t = 7.7 s, the results were closer to those obtained by Bouscasse et al. [7], with a relative error of 7.78%. For roll, it is observed that for the time instants t = 7.5 s and 7.9 s the results are closer to the results of Hadžić et al. [6], with relative errors of 8.98% and 12%, respectively. Figure 6 presents free surface configurations obtained here for some time instants during the present simulation.

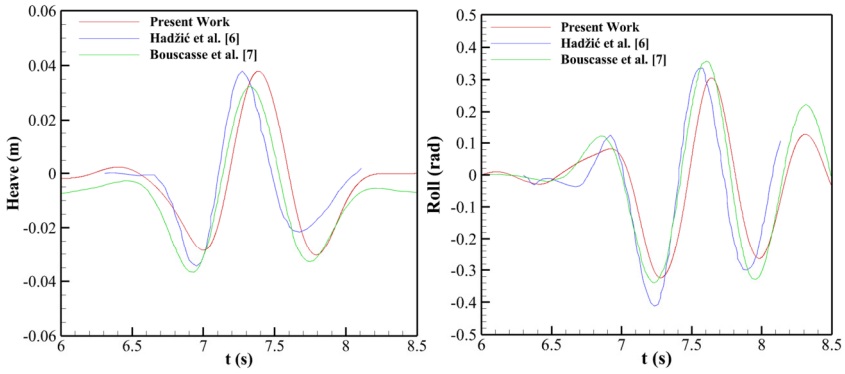

Figure 5. Time histories related to heave and roll motions, wave packet interacting with floating body

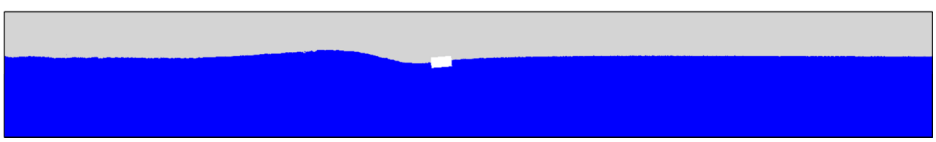

(continues on next page)

Figure 6. Free surface configurations over time, wave packet interacting with floating body

3.2 Floating body with mooring

Initially proposed by Gunn et al. [8], this problem presents a spherical buoy anchored by a vertical cable, as shown in Fig. 7. The buoy is originally submerged by 15 mm (relative to its top) and then released, floating vertically until it reaches a state of equilibrium at rest.

The sphere has a mass of 1.745 kg and a radius of 101.5 mm. The buoy is made from a hollow sphere with high density expanded polystyrene (density of 29.5 kg m^{-3}) with 40 mm thickness (Gunn et al. [8]). To ensure that the center of mass is located below the centroid (thus ensuring a stable sitting orientation in the water) a 38 mm thick mild steel disk with a radius of 40 mm was placed in the lower half of the buoy, which lowered the center of mass 27 mm in relation to the centroid (see Gunn et al. [8] for additional information). The moments of inertia I_{xx}, I_{yy}, I_{zz} are 1.7352 kg m², 1.7764 kg m² and 1.7352 kg m², respectively.

The anchor cable has a diameter of 1 mm. In the experimental study, a spring was used to represent the stiffness of the mooring cable. To avoid damping in its expansion and contraction movements, the spring was placed out of the water, with stiffness of 30.88 N m^{-1}, which was numerically simulated in this work by choosing an appropriate modulus of elasticity for the cable.

For the numerical model, a computational domain with 1 m length, 1 m width and 1.6 m tall was adopted, which is based on the numerical model utilized by Gunn et al. [8]. To avoid the effect of bouncing waves, a sponge layer of 0.15 m length L_s and damping intensity parameter $\alpha_s = 400$ was used. Two meshes were utilized in this study: Mesh 1 – 1,342,130 elements and 240,423 nodes, with a smallest element length of 2 x 10^{-3} m; Mesh 2 – 816,516 elements and 142,047 nodes, with a smallest element length of 1 x 10^{-2} m.

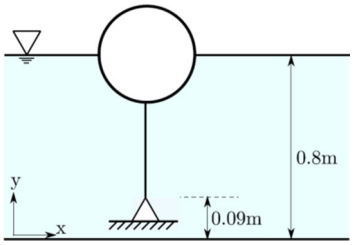

Figure 7. General scheme, floating buoy with mooring

Figure 8 presents results referring to the cable positions over time, which are compared with experimental results obtained by Gunn et al. [8]. Note the proximity between both predictions, although the result obtained with the model proposed in this work shows a lower damping over time. For Mesh 1, an average relative error of 2.5% was observed relative to the reference results and a maximum relative error of 2.86% at the time instant t = 1.76 s was identified. As for Mesh 2, there was an average relative error in the order of 1.5% relative to the reference results and the highest relative error of 4.26% was observed at t = 0.33 s.

In order to better simulate the damping effect induced by cable-pulley interactions in the experimental study, new simulations were carried out with Mesh 2, considering a critical damping ratio of 15%. From the results, it is observed that the present solution approximated better the experimental result, with an average relative error of the order of 1% and a maximum relative error of 2.5% at the time instant t = 0.33 s. Considering that the buoy vertical motion showed a well-behaved attenuation over time, it can also be concluded that the numerical sponge used here was able to satisfactorily avoid the reflection of waves in the flow field. Finally, Fig. 8 also shows free surface configurations obtained here for some time instants.

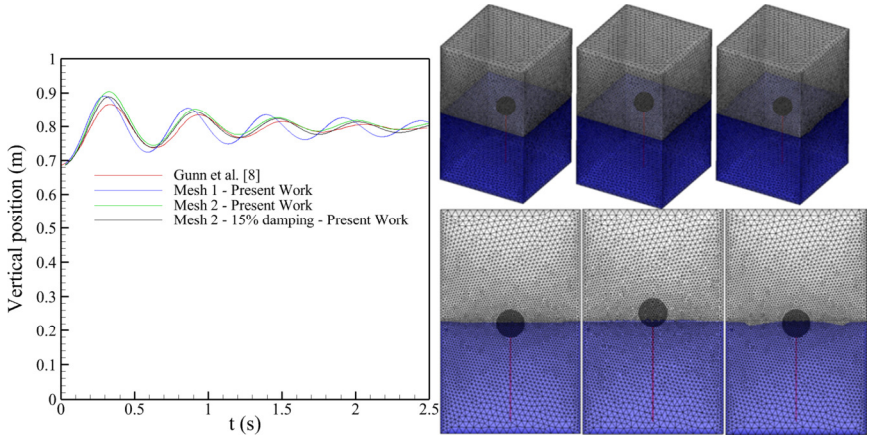

Figure 8. Buoy vertical motion over time and free surface configurations, floating buoy with mooring

4 Conclusions

In this work a numerical model for FSI analysis of floating objects with mooring was developed. From the results obtained, it was observed that the CBS semi-implicit scheme adopted here proved to be numerically stable, presenting accurate predictions for free surface flow applications. A cable formulation based on NPFEM was utilized here for cable dynamics, obtaining results very similar to those presented by reference works. It was also observed that the Level Set method was successfully applied to complex problems involving two-phase free surface flows. Finally, the partitioned coupling scheme proposed in this work was validated using numerical simulation of experimental applications, including complex problems of floating objects with and without mooring cable, where accurate predictions were obtained with the present model.

Acknowledgements. The authors would like to thank CNPq and CAPES for their financial support to this ongoing research. This research was developed with the support of the Núcleo Avançado de Computação de Alto Desempenho (NACAD) – COPPE, Universidade Federal do Rio de Janeiro (UFRJ); Centro Nacional de Processamento de Alto Desempenho em São Paulo (CENAPAD-SP); and Laboratório Nacional de Computação Científica (LNCC).

Authorship statement. The authors hereby confirm that they are the sole liable persons responsible for the authorship of this work, and that all material that has been herein included as part of the present paper is either the property (and authorship) of the authors, or has the permission of the owners to be included here.

References

[1] P. R. F. Teixeira. *Simulação numérica da interação de escoamentos tridimensionais de fluídos compressíveis e incompressíveis e estruturas deformáveis usando o Método dos Elementos Finitos*. PhD thesis, UFRGS, 2001.
[2] F. J. Sun, Z. H. Zhu and M. Larosa, "Dynamic modeling of cable towed body using nodal position finite element method". *Ocean Engineering*, vol. 38, pp. 529–540, 2011.
[3] M. Sussman, A. S. Almgren, J. B. Bell, P. Colella, L. H. Howell and M. L. Welcome, "An adaptive Level Set approach for incompressible two-phase flows". *Journal of Computational Physics*, vol. 148, pp. 81–124, 1999.
[4] M. Sussman, P. Smereka and S. Osher, "A level set approach for computing solutions to incompressible two-phase flow". *Journal of Computational Physics*, vol. 114, pp. 146–159, 1994.
[5] Z. H. Zhu, "Dynamic modeling of cable system using nodal position finite element method". *International Journal for Numerical Methods in Biomedical Engineering*, vol. 26, pp. 692–704, 2010.
[6] I. Hadžić, J. Henning, M. Perić and Y. Xing-Kaeding, "Computation of flow-induced motion of floating bodies". *Applied Mathematical Modeling*, vol. 29, pp. 1196–1210, 2005.
[7] B. Bouscasse, A. Colagrossi, S. Marrone and M. Antuono, "Nonlinear water wave interaction with floating bodies in SPH". *Journal of Fluids and Structures*, vol. 42, pp. 112–129, 2013.
[8] D. F. Gunn, M. Rudman and R. C. Z. Cohen, "Wave interaction with a tethered buoy: SPH simulation and experimental validation". *Ocean Engineering*, vol. 156, pp. 306–317, 2018.